



# Revisiting the quasinormal modes of the Schwarzschild black hole: Numerical analysis

Luis A. H. Mamani<sup>1,2,3,a</sup>, Angel D. D. Masa<sup>4,5,b</sup>, Lucas Timotheo Sanches<sup>4,c</sup>, Vilson T. Zanchin<sup>4</sup>

<sup>1</sup> Centro de Ciências Exatas e Tecnológicas, Universidade Federal do Recôncavo da Bahia, Rua Rui Barbosa, 710, Cruz das Almas, Bahia 44380-000, Brazil

<sup>2</sup> Laboratório de Astrofísica Teórica e Observacional, Departamento de Ciências Exatas e Tecnológicas, Universidade Estadual de Santa Cruz, Ilhéus, Bahia 45650-000, Brazil

<sup>3</sup> Centro de Ciências Exatas Naturais e Tecnológicas, Universidade Estadual da Região Tocantina do Maranhão, Rua Godofredo Viana 1300, Imperatriz, Maranhão 65901-480, Brazil

<sup>4</sup> Centro de Ciências Naturais e Humanas, Universidade Federal do ABC, Avenida dos Estados 5001, Santo André, São Paulo 09210-580, Brazil

<sup>5</sup> Departamento de Física, Facultad de Ciencias Exactas y Naturales, Universidad de Cartagena, Carrera 50 # 24-120, Cartagena de Indias, Bolívar 130015, Colombia

Received: 18 August 2022 / Accepted: 28 September 2022 / Published online: 10 October 2022  
© The Author(s) 2022

**Abstract** We revisit the problem of calculating the quasinormal modes of spin 0, 1/2, 1, 3/2, 2, and spin 5/2 fields in the asymptotically flat Schwarzschild black hole spacetime. Our aim is to investigate the problem from the numerical point of view, by comparing some numerical methods available in the literature and still not applied for solving the eigenvalue problems arising from the perturbation equations in the Schwarzschild black hole spacetime. We focus on the pseudo-spectral and the asymptotic iteration methods. These numerical methods are tested against the available results in the literature, and confronting the precision between each other. Besides testing the different numerical methods, we calculate higher overtones quasinormal frequencies for all the investigated perturbation fields in comparison with the known results. Additionally, we obtain purely imaginary frequencies for spin 1/2 and 3/2 fields that are in agreement with analytic results reported previously in the literature. The purely imaginary frequencies for the spin 1/2 perturbation field are exactly the same as the frequencies obtained for the spin 3/2 perturbation field. In turn, the quasinormal frequencies for the spin 5/2 perturbation field are calculated for the very first time, and purely imaginary frequencies are found also in this case. We conclude that both methods provide accurate results and they complement each other.

## 1 Introduction

Perturbation theory is a very useful theoretical toolkit for the investigation of the properties of a physical system. For example, the stability under small perturbations. Investigating the harmonic oscillator problem, it drives into a second-order differential equation with Dirichlet boundary conditions whose solutions are characterized by a set of discrete real frequencies, i.e., normal modes (NMs). However, there are physical systems whose boundary conditions drive solutions with complex frequencies, i.e., quasinormal modes (QNMs), for example, a harmonic oscillator into a dissipative medium, see for instance [1]. Thus, the investigation of the quasinormal (QN) frequencies and their mathematical properties become a fascinating subject that may shed light on the understanding of the universal properties of the physical system under investigation.

In the context of gravity theories, perturbation theory is essential for several reasons. One of the motivations is the investigation of gravitational waves spectroscopy [2]. One also may use perturbation theory to investigate the stability of physical systems under small perturbations. It has been shown that the perturbation equations may be written as second-order differential equations, allowing us to use numerical techniques implemented in differential equations to solve them. One of the boundary conditions considers that classically nothing comes out from the black hole interior such that the boundary conditions at the horizon are ingoing waves. In turn, at the spatial infinity the boundary conditions are outgoing waves because nothing can come from

<sup>a</sup> e-mail: alex.h.mamani@gmail.com (corresponding author)

<sup>b</sup> e-mail: angel.masa@ufabc.edu.br

<sup>c</sup> e-mail: lucas.t@ufabc.edu.br

outside of the spacetime. Solving the perturbation equations under these particular boundary conditions drive to solutions with discrete (complex) eigenvalues. Such eigenvalues are the frequencies representing the characteristic oscillations of the black hole that relaxes after being perturbed. One very essential property of these frequencies is that they do not depend on the initial condition (perturbation) and are fixed completely by the properties of the black hole under investigation.

The quasinormal modes are of particular interest in black hole astrophysics. Direct observations showed in the coalescence of a binary system emits gravitational waves in the form of QNMs, that is, the final system obeys the predictions of black hole perturbation theory [3]. This fact alone is enough to motivate the development, testing, and comparison of different methods for finding QNMs, but the relevance of QNMs go far further than this fact. For reviews and additional discussions about QNMs in different contexts see, for instance, [4–28] and references therein.

In turn, the first observation of the shadow of the supermassive black hole M87\* by the Event Horizon Telescope Collaboration (EHT) [29,30] opens a new window for the investigation of strong gravitational field phenomena. There is also studies proposing a connection between the real part of the quasinormal (QN) frequency with the radius of the shadow, see the Refs. [31–35]. Among the new possibilities, there are researched papers attempting to find constraints in parameters arising in different models like in general uncertainty principle (GUP), see for instance, refs. [36,37].

In this paper we revisit the calculation of quasinormal modes for integer spin 0, 1 and 2 fields, as well as for semi-integer spin 1/2, 3/2 and 5/2 fields. Since Chandrasekhar calculated the quasinormal modes for  $s = 2$  in Ref. [38], the problem of calculating QNMs for other spin fields was previously investigated in the literature using different techniques (numeric and analytic), see for instance, Refs. [39–44]. However, our approach here is from the numerical point of view, for doing so we are going to use two numerical methods well established in the literature. The first one is the pseudo-spectral method used to solve differential equations expanding the solution in a base composed of special functions [45]. The pseudo-spectral method, was used to calculate the quasinormal modes of Schwarzschild black hole for spin-zero fields in Ref. [46]. However, we extend the method for calculating the QNMs for spin 1/2, 1, 3/2, 2, and 5/2 fields. We also use the asymptotic iteration method (AIM) proposed originally in Ref. [47]. This method was extended to solve quasinormal modes in Ref. [43]. In the present paper, we review the relatively unexplored asymptotic iteration method and apply it to the QNM problem. We also introduce a new software package that implements the latter method for usage in general second-order ordinary differential equations (ODEs).

The paper is organized as follows. In Sect. 2 we write the equations of motion describing the spin 0, 1/2, 1, 3/2, 2, and 5/2 perturbation fields in a suitable form to apply the numerical methods. In Sect. 3, we review and discuss the pseudo-spectral method, focusing on the way in which this method can be applied, by expanding the solution using one or two special functions. Section 4 is devoted for discussing the AIM and its extensions to calculate QN frequencies. We also present an open-source code that can be used freely. In turn, in Sect. 5 we present our numerical results obtained in both methods, we also compare against numerical results available in the literature. We leave the discussion of the QNMs in the limit of large angular momentum for Sect. 6, where we also compare against analytic results. Finally, our conclusions are presented in Sect. 7. Additional details are presented in Appendix A and Appendix B.

## 2 Equations of motion

Here we write the equations describing the field perturbations on the gravitational background solution of the Einstein equations. We focus on the metric for a spherically symmetric black hole, which is given by [48]

$$ds^2 = -f(r) dt^2 + \frac{1}{f(r)} dr^2 + r^2 d\theta^2 + r^2 \sin^2 \theta d\varphi^2, \quad (1)$$

where the horizon function of the Schwarzschild black hole is given by

$$f(r) = 1 - \frac{2M}{r}. \quad (2)$$

where  $M$  is the mass of the black hole, and  $r$  is the radial coordinate which, in principle, belongs to the interval  $r \in [0, \infty)$ . The coordinates in the metric (1) are known as Schwarzschild coordinates. As it is well known, this metric presents an event horizon at  $r = 2M$  and a curvature (physical) singularity at  $r = 0$ . In the asymptotic region, i.e.,  $r \rightarrow \infty$ , the metric reduces to a flat metric. As long as the quasinormal modes in this black hole spacetime are concerned, the interesting region is the spacetime region spanned by the radial coordinate  $r$  in the interval  $2M < r < \infty$ .

We then follow the standard procedure in the study of linear perturbations of the Schwarzschild black hole spacetime (1). After chosen an specific perturbation field, the corresponding partial differential equations are reduced to a unique Schrödinger like ordinary differential equation for each field through a set of transformations. In such an approach, the perturbation functions are decomposed in Fourier modes, in the form  $e^{i\omega t} = e^{i(\omega_{Re} - i\omega_{Im})t} = e^{\omega_{Im} t} \cos(\omega_{Re} t)$ , what eliminates the time derivatives from the differential equations, while the angular dependence is dealt with by expanding in spherical harmonics as usual.

As a final remark at this stage we mention that ordinary QNM present frequencies with non-vanishing real and imaginary parts and represent oscillatory solutions, being exponentially damped by the imaginary part of the frequency. On the other hand, the modes with purely imaginary frequencies, i.e., the modes for which the real part of the frequency vanishes, represent purely damping solutions because the respective perturbation functions go as  $e^{i\omega t} = e^{\omega_{Im} t}$ .

### 2.1 Spin 0, 1 and 2 perturbations

Here we revisit the study of perturbations of integer spin, such that scalar, vector, and gravitational perturbations in the Schwarzschild black hole spacetime. This is a long-standing problem, and there are a considerable amount of results published in the literature, which is certainly interesting for one of the purposes of the present work. In fact, it was proven that the equations of motion can be written in a compact form, the so-called, Schrödinger-like differential equations, see for instance [4]. Thus, for massless scalar ( $s = 0$ ), electromagnetic ( $s = 1$ ) and vector type gravitational perturbations ( $s = 2$ ), the Schrödinger-like equations are given by

$$\frac{d^2 \psi_s(r)}{dr_*^2} + [\omega^2 - V_s(r)] \psi_s(r) = 0. \tag{3}$$

where the potential is given by

$$V_s(r) = f(r) \left[ \frac{\ell(\ell + 1)}{r^2} + (1 - s^2) \frac{2M}{r^3} \right], \tag{4}$$

where the tortoise coordinate is defined in terms of the areal coordinate  $r$  by  $dr_* = dr/f(r)$ . So far, the problem of calculating quasinormal frequencies was reduced to solve an eigenvalue problem. We will see that it is possible to solve this problem following two approaches, one of them expanding the function  $\psi$  in a base composed of special functions, while the other solving directly the second-order differential equation.

On the other hand, note that the potential (4) is zero at the horizon,  $f(r_h) = 0$ . Thus, the Schrödinger-like equation reduces to a single harmonic oscillator problem, whose solutions are:

$$\psi_s(r) = c_1 e^{-i\omega r_*} + c_2 e^{i\omega r_*}, \quad r \rightarrow r_h. \tag{5}$$

The first of these solutions is interpreted as an ingoing wave, i.e., a wave that travels inward and eventually falls into the black hole event horizon. The second solution is interpreted as an outgoing wave, i.e., a wave that travels outward with respect to the black hole and can escape to space infinity. Waves travelling as this second solution would represent waves coming from the interior of the black hole. Since the perturbation theory is implemented using classical assumptions, nothing is expected to come out from the black hole interior, thus, in the following analysis we impose the first

solution as boundary condition at the horizon what is accomplished by setting  $c_2 = 0$ .

We also need to investigate the spatial infinity, at  $r \rightarrow \infty$ , where  $f(r) \rightarrow 1$  and the effective potential (4) also vanishes. Thus, in such a limit the general solutions to the wave equation (3) have the same form as the function given in Eq. (5), i.e.,

$$\psi_s(r_*) = c_3 e^{-i\omega r_*} + c_4 e^{i\omega r_*}, \quad r \rightarrow \infty. \tag{6}$$

The first solution is interpreted physically as waves coming in from outside the universe and must be avoided by setting  $c_3 = 0$ . In turn, the second solution represents waves going out of the universe, this is the boundary condition at the spatial infinity. Finally, note that the boundary conditions do not depend explicitly on the angular momentum  $\ell$  nor the spin.

It is interesting to see the behavior of the tortoise coordinate close to the horizon which is given by

$$r_* = \int \frac{dr}{f'(r_h)(r - r_h)} \approx \frac{\ln(r - r_h)}{f'(r_h)}, \quad r \rightarrow r_h \tag{7}$$

where  $r_h = 2M$ . Thus, in terms of the radial coordinate, the boundary condition at the horizon becomes ( $f'(r_h) = 1/r_h$ )

$$\psi_s(r) \sim e^{-i\omega \frac{\ln(r-r_h)}{f'(r_h)}} \sim (r - r_h)^{-i \frac{\omega}{f'(r_h)}}. \tag{8}$$

In turn, the tortoise coordinate at the spatial infinity becomes

$$r_* = \int \frac{dr}{f(r)} \approx r + r_h \ln r, \quad r \rightarrow \infty \tag{9}$$

while the asymptotic solution at the spatial infinity becomes

$$\psi_s(r) \sim e^{i\omega(r+r_h \ln r)} \sim r^i r_h \omega e^{i\omega r}. \tag{10}$$

In the following, we are going to change our strategy and use a new coordinate defined by  $u = 2M/r$ . This is equivalent to the choice  $u = 1/r$  and then normalizing the mass  $M$  to  $2M = 1$ . The relation between the tortoise coordinate  $r_*$  and the new coordinate  $u$  becomes  $du/dr_* = -u^2 f(u)$ .

We also constrained our analysis to the outer region of the black hole, such that  $r_h \leq r < \infty$ . Hence, in terms of the new coordinate, this region is bounded to the interval  $u \in [0, 1]$ , and the potential becomes

$$V_s(u) = f(u) u^2 \left[ \ell(1 + \ell) + (1 - s^2) u \right], \tag{11}$$

where  $f(u) = 1 - u$ .

To implement the pseudo-spectral method, the equations on the background metric must be written in terms of the Eddington–Filkenstein coordinates, see for instance the discussion in Ref. [46]. However, we found a short way to write the equations going directly from the Schrödinger-like equation by implementing some transformations. In the end, these transformations lead to a differential equation, which is the same as the one obtained from the metric in Eddington–Filkenstein coordinates. To write the perturbation equations

in terms of the Eddington–Filkenstein coordinates we must implement the transformation  $\psi_s \rightarrow \Phi_s$  given by

$$\psi_s = \frac{\Phi_s(u)}{u} e^{-i\omega r_*(u)}. \tag{12}$$

Thus, Eq. (3) becomes

$$\left[ s^2 u^2 - \ell(\ell + 1)u - 2i \right] \Phi_s(u) - u \left( u^2 - 2i \right) \Phi'_s(u) + (1 - u) u^3 \Phi''_s(u) = 0, \tag{13}$$

where we have set  $M = 1/2$  so that  $r_h = 1$ . The asymptotic solutions close to the horizon may be calculated using the ansatz  $\Phi_s(u) = (1 - u)^\alpha$ . By substituting this ansatz into (13) we get two solutions,

$$\alpha = 0, \quad \alpha = 2i \omega. \tag{14}$$

The solution for  $\alpha = 0$  is interpreted physically as the ingoing waves at the horizon, while the other one is interpreted as a wave coming out from the black hole interior. Therefore, the second solution must be neglected in the following analysis.

In the same way, we consider the ansatz  $\Phi_s = u^\beta$  to get the asymptotic solution close to the spatial infinity. Plugging this ansatz in (13) we get the following solution,

$$\Phi_s(u) = c_5 e^{2i\omega/u} u^{-2i\omega} + c_6 u. \tag{15}$$

We want the divergent solution, such that we set  $c_6 = 0$ . Then, we implement the final transformation, which takes into consideration the boundary conditions,

$$\Phi_s(u) = e^{2i\omega/u} u^{-2i\omega} \phi_s(u), \tag{16}$$

where  $\phi_s(u)$  is a regular function in the interval  $u \in [0, 1]$  by definition. Finally, the equation of motion describing spin 0, 1, and 2 perturbations is given by

$$\left[ \ell(\ell + 1)u - s^2 u^2 - 4i\lambda - 16u(1 + u)\lambda^2 \right] \phi_s(u) + \left[ u^3 + 4iu(1 - 2u^2)\lambda \right] \phi'_s(u) - (1 - u)u^3 \phi''_s(u) = 0, \tag{17}$$

where we have used  $\lambda = \omega M = \omega/2$ . The final differential equation is then a quadratic eigenvalue problem in  $\lambda$ . It is worth also mentioning that in the limit of zero spin  $s \rightarrow 0$ , Eq. (17) reduces to Eq. (4.8) of Ref. [46]. These results just prove that the alternative way for getting the equations for the integer spin perturbations presented here is consistent with other approaches found in the literature.

The differential equation (17) was solved numerically using the pseudo-spectral and AIM methods. The results for perturbations of spin 0, 1, and 2 are presented in Sects. 5.1, 5.2, and 5.3, respectively, where a comparison with the corresponding data in the literature is also performed.

In the following, we extend the analysis of the present section to other kinds of perturbations.

## 2.2 Spin 1/2 perturbations

For half-integer spin perturbations the history is different, the differential equations are quite distinct from (17). The equation for the spin 1/2 Dirac field as a perturbation on the Schwarzschild background was derived in Ref. [40] by using the Newman–Penrose formalism. The analysis was generalized for arbitrary half-integer spin in Ref. [41]. The resulting equation of motion for the perturbations may be written in the Schrödinger-like form Eq. (3), where the potential for the massless spin 1/2 field is given by

$$V_{1/2} = \frac{(1 + \ell) \sqrt{f(r)}}{r^2} \left[ (1 + \ell) \sqrt{f(r)} + \frac{3M}{r} - 1 \right]. \tag{18}$$

It is worth mentioning that we have found a typo in the definition of  $\Delta$  in [40], which must be  $\Delta = r(r - 2M)$ .

We then implement the same transformations done in the integer spin cases. First, we change the radial coordinate to  $u = 2M/r$ , which is defined in the interval  $u \in [0, 1]$ . Then by setting  $2M = 1$  the effective potential (18) becomes

$$V_{1/2} = (1 + \ell) u^2 \sqrt{f(u)} \left[ (1 + \ell) \sqrt{f(u)} + \frac{3u}{2} - 1 \right]. \tag{19}$$

It is interesting pointing out that the asymptotic solutions do not depend on the spin of the field, for that reason the asymptotic solutions for this problem are the same as those obtained in Eqs. (14) and (15). Then, similar transformations as those given in Eqs. (12) and (16) can be applied also in the present spin 1/2 case. Thus, the differential equation to be solved is given by

$$R(u)\phi_{1/2}(u) + Q(u)\phi'_{1/2}(u) + P(u)\phi''_{1/2}(u) = 0, \tag{20}$$

in which the coefficients  $R(u)$ ,  $Q(u)$ , and  $P(u)$  are given by

$$R(u) = u^3 + u(1 + \ell) \left( 1 + \ell - \sqrt{1 - u} \right) + \frac{u^2}{2} \left[ (1 + \ell) \left( 3\sqrt{1 - u} - 4 \right) - 2\ell^2 \right] - 4i(1 - u)\lambda - 16u(1 - u^2)\lambda^2, \tag{21}$$

$$Q(u) = u^3(1 - u) + 4iu\lambda \left( 1 - u - 2u^2 + 2u^3 \right), \tag{22}$$

$$P(u) = -u^3(1 - u)^2, \tag{23}$$

respectively, and with  $\lambda$  standing for  $\lambda = M\omega = \omega/2$ .

As can be seen, the differential equation (20) is impregnated by square roots that may difficult the convergence of the numerical methods. To avoid the square roots, we implement an additional change of variable  $\chi^2 = 1 - u$ . Nevertheless, the new coordinate also belongs to the interval  $\chi \in [0, 1]$ . The differential equation (20) becomes

$$R(\chi)\phi_{1/2}(\chi) + Q(\chi)\phi'_{1/2}(\chi) + P(\chi)\phi''_{1/2}(\chi) = 0, \tag{24}$$

in which the coefficients  $R(\chi)$ ,  $Q(\chi)$ , and  $P(\chi)$  are given by

$$R(\chi) = 2(1 - \chi^2) [(\ell + 1) \times (1 + 2\ell\chi - 3\chi^2) + 2\ell\chi + 2\chi^3] - 8i\chi\lambda - 32\chi(2 - 3\chi^2 + \chi^4)\lambda^2, \tag{25}$$

$$Q(\chi) = (\chi^2 - 1) [(1 - \chi^2)^2 - 8i(1 - 4\chi^2 + 2\chi^4)\lambda], \tag{26}$$

$$P(\chi) = -\chi(1 - \chi^2)^3. \tag{27}$$

In Sect. 5.4 we solve Eq. (24) by using the pseudo-spectral and AIM methods and compare our results against the results of Refs. [40,41].

### 2.3 Spin 3/2 perturbations

As well as for the spin 1/2 perturbation field, the perturbation equation for spin the 3/2 field is quite different from the integer spin fields. To get the relevant equation we use the result obtained in Ref. [41], specifically Eq. (37) of that reference, and by setting  $s = 3/2$  on such an equation we get the effective potential of the Schrödinger-like equation (3),

$$V_{3/2} = \frac{(1 + \ell)(2 + \ell)(3 + \ell)\sqrt{f(r)}}{[2M + r(1 + \ell)(3 + \ell)]^2} \left( \frac{2M^2}{r^2} + (1 + \ell)(3 + \ell) \times \left[ (2 + \ell)\sqrt{f(r)} + \frac{3M}{r} - 1 \right] \right). \tag{28}$$

As before, we change the radial coordinate to  $u = 1/r$  and consider  $2M = 1$ . Thus, the potential becomes

$$V_{3/2} = \frac{u^2(1 + \ell)(2 + \ell)(3 + \ell)\sqrt{1 - u}}{2[u + (1 + \ell)(3 + \ell)]^2} \left( \frac{u^2}{2} + (1 + \ell)(3 + \ell) \times \left[ (2 + \ell)\sqrt{1 - u} + \frac{3u}{2} - 1 \right] \right). \tag{29}$$

Following the procedure implemented from Eqs. (12)–(15), where we go from the Schrödinger-like equation to a differential equation suited to the numerical methods we are working with, the differential equation (20) becomes

$$R(\chi)\phi_{3/2}(\chi) + Q(\chi)\phi'_{3/2}(\chi) + P(\chi)\phi''_{3/2}(\chi) = 0, \tag{30}$$

where the coefficients  $R(\chi)$ ,  $Q(\chi)$ , and  $P(\chi)$  are given by

$$R(\chi) = 2(1 - \chi^2) [6 + 11\ell + 6\ell^2 + \ell^3 + 2\chi^5 + 4\chi^4(2 + \ell) + 2\chi^3(3 + 4\ell + \ell^2) - \chi^2(2 - 7\ell - 6\ell^2 - \ell^3) + 2\chi(2 + \ell)^2(2 + 4\ell + \ell^2) - 16\chi(2 + \chi + \ell)^2\lambda [i + 4(2 - \chi^2)(1 - \chi^2)\lambda],$$

$$Q(\chi) = -(1 - \chi^2)(2 + \chi + \ell^2) \times [(1 - \chi^2)^2 - 8i(1 - 4\chi^2 + 2\chi^4)\lambda],$$

$$P(\chi) = -\chi(1 - \chi^2)^3(2 + \chi + \ell)^2.$$

where we have used the new coordinate  $\chi^2 = 1 - u$  to avoid square roots. Again, we get a quadratic eigenvalue problem, and the function  $\phi_{3/2}(\chi)$  is regular in the interval  $\chi \in [0, 1]$ . In Sect. 5.5 we solve Eq. (30) by using the pseudo-spectral and AIM methods and compare our results against the results of Refs. [41,49].

### 2.4 Spin 5/2 perturbations

It is believed that the investigation of higher spin fields may shed some light on the understanding of fundamental physics, like on new unifying theories for the fundamental interactions, or new phenomenology beyond the standard model. The main motivation for investigating the spin 5/2 field perturbation is the Rarita–Schwinger theory. Inspired by such a theory, the authors of Ref. [50] computed some physical observable for the spin  $\frac{5}{2}$ -field. In this section, we use the generic equation obtained in Ref. [41], specifically Eq. (37), to determine the quasinormal frequencies of this perturbation field on the Schwarzschild black hole. The differential equation for the perturbations becomes so complicated, for that reason, we write it in Appendix A. The resulting equation is solved numerically by using the pseudo-spectral and AIM methods. The numerical results are displayed in Sect. 5.6.

## 3 The pseudo-spectral method

It is well known that the Fourier method is appropriate to solve periodic problems. Nevertheless, it cannot be applied for nonperiodic problems due to the Gibbs phenomenon arising at the boundaries [51]. An alternative method to solve nonperiodic problems is the pseudo-spectral method, which recently has been applied to solve differential equations numerically in many problems. The fact that the coordinate domain is not periodic,  $u \in [0, 1]$ , leads us to use this method in the present problem. Note that the quadratic eigenvalue problem can be written in the form (using the notation of Ref. [46]),

$$c_0(u, \lambda, \lambda^2)\phi + c_1(u, \lambda, \lambda^2)\phi' + c_2(u, \lambda, \lambda^2)\phi'' = 0. \tag{31}$$

where  $\phi$  is a function of the coordinate  $u$  alone and primes indicate derivatives with respect to  $u$ . The coefficients of this equation can be written as  $c_j(u, \lambda, \lambda^2) = c_{j,0}(u) + \lambda c_{j,1}(u) + \lambda^2 c_{j,2}(u)$ , where  $c_{j,0}(u)$ ,  $c_{j,1}(u)$ , and  $c_{j,2}(u)$  are polynomials of  $u$  only.

The idea behind the pseudo-spectral method is to rewrite the regular function  $\phi(u)$  in a base composed of cardinal functions,  $C_j(u)$ , in the form

$$\phi_s(u) = \sum_{j=0}^N g(u_j) C_j(u), \tag{32}$$

where  $g(u)$  is a function of  $u$ . The next step is to evaluate the differential equation (including these functions) on a grid or collocation points. The best choice is the Gauss–Lobato grid given by

$$u_i = \frac{1}{2} \left( 1 \pm \cos \left[ \frac{i}{N} \pi \right] \right), \quad i = 0, 1, 2, \dots, N \tag{33}$$

Note that (33) maps the interval  $[-1, 1]$  into  $[0, 1]$ .

Evaluating on the grid, the polynomials of (31) become elements of a matrix  $c_j(u_i, \lambda, \lambda^2) = c_{j,0}(u_i) + \lambda c_{j,1}(u_i) + \lambda^2 c_{j,2}(u_i)$ . Then, the matrix representation of the quadratic eigenvalue problem (31) can be written as

$$\left( \tilde{M}_0 + \tilde{M}_1 \lambda + \tilde{M}_2 \lambda^2 \right) g = 0, \tag{34}$$

where

$$\begin{aligned} (\tilde{M}_0)_{ji} &= c_{0,0}(u_i) D_{ji} + c_{1,0}(u_i) D_{ji}^{(1)} + c_{2,0}(u_i) D_{ji}^{(2)}, \\ (\tilde{M}_1)_{ji} &= c_{0,1}(u_i) D_{ji} + c_{1,1}(u_i) D_{ji}^{(1)} + c_{2,1}(u_i) D_{ji}^{(2)}, \\ (\tilde{M}_2)_{ji} &= c_{0,2}(u_i) D_{ji} + c_{1,2}(u_i) D_{ji}^{(1)} + c_{2,2}(u_i) D_{ji}^{(2)}, \end{aligned} \tag{35}$$

here  $D_{ji}$ ,  $D_{ji}^{(1)}$ , and  $D_{ji}^{(2)}$  represent the cardinal function and its derivatives. Defining  $\tilde{g} = \lambda g$ , the last equation may be written in the form

$$\tilde{M}_0 g + \left( \tilde{M}_1 + \tilde{M}_2 \lambda \right) \tilde{g} = 0, \tag{36}$$

This is the first step to linearize the quadratic eigenvalue problem. For a generalization of this procedure see for instance Ref. [52]. Therefore, the matrix representation of the eigenvalue problem may be written as

$$(M_0 + M_1 \lambda) \cdot \tilde{g} = 0, \tag{37}$$

where we have defined the new matrices

$$M_0 = \begin{pmatrix} \tilde{M}_0 & \tilde{M}_1 \\ 0 & \mathbb{1} \end{pmatrix}, \quad M_1 = \begin{pmatrix} 0 & \tilde{M}_2 \\ -\mathbb{1} & 0 \end{pmatrix}, \quad \tilde{g} = \begin{pmatrix} g \\ \tilde{g} \end{pmatrix}. \tag{38}$$

Notice that  $M_0$  and  $M_1$  are  $(N + 1) \times (N + 1)$  matrices and  $\tilde{g}$  is a  $(N + 1)$ -dimensional vector with components  $g_j = g(u_j)$ ,  $j = 0, 1, \dots, N$ . Finally, the QN frequencies are determined by solving the linear system (37). The procedure is described here for a quadratic eigenvalue problem, but it can be easily extended to arbitrary order in the eigenvalues whenever the power of the frequency is an integer. However, in cases where the value of the effective potential changes at the spatial infinity, as in the case of a massive scalar field, see for instance [53], the implementation of the pseudo-spectral method is not obvious because the power of the frequency turns out semi-integer such that it is not possible to write the eigenvalue problem in the form of Eq. (34).

Having described the procedure to calculate the eigenvalues, we need to specify the cardinal functions. We realized that these functions must depend on one or more Chebyshev polynomials of the first kind  $T_k(u)$ . In the following, we consider two forms for the cardinal functions. The first model takes into consideration one Chebyshev polynomial in the form,

$$C_j(u) = T_j(u). \tag{39}$$

We call this particular choice pseudo-spectral I. The second model considers two Chebyshev polynomials [46]

$$C_j(u) = \frac{2}{N p_j} \sum_{m=0}^N \frac{1}{p_m} T_m(u_j) T_m(u), \quad \begin{cases} p_0 = 2, \\ p_N = 2, \\ p_j = 1. \end{cases} \tag{40}$$

We call this choice pseudo-spectral II. It is worth mentioning that the pseudo-spectral method inevitably leads to the emergence of spurious solutions that do not have any physical meaning. To eliminate the spurious solutions we use the fact that the relevant QN frequencies do not depend on the number of Chebyshev polynomials being considered. An additional check of consistency is to plot the eigen-functions  $\phi_s(u)$ , which must satisfy the boundary conditions, i.e.,  $\phi_s(u)$  must be regular in the interval  $u \in [0, 1]$ . Note that the problem of calculating QN frequencies does not depend on any initial guess, such as the shooting method, for example. We get directly the frequencies by using, for instance, Mathematica’s built-in function Eigenvalues, or Eigensystem. One may consider this fact as an advantage in relation to other methods available in the literature.

Finally we mention that the Chebyshev polynomials of the first kind  $T_k(x)$  are defined in the interval  $x \in [-1, 1]$ , and have special properties [51], but the collocation points (33) map this interval into the interval of interest, i.e.,  $u \in [0, 1]$ . In turn, the error associated with the pseudo-spectral method is of the order  $\mathcal{O}(1/N^N)$  for sufficiently smooth regular functions [54]. For further details on this subject, see for instance Ref. [46].

#### 4 The asymptotic iteration method

The asymptotic iteration method (AIM) is a numerical method recently proposed in Ref. [47] for solving homogeneous second-order ordinary differential equations of the form,

$$y''(x) - \lambda_0(x) y'(x) - s_0(x) y(x) = 0, \tag{41}$$

where primes denote derivatives with respect to the variable  $x$  (that is defined over some interval that is not necessarily bounded),  $\lambda_0(x) \neq 0$  and  $s_0(x)$  are  $C_\infty$ . These equations can

be found in many different areas of physics, such as the time-independent Schrödinger equation in Quantum Mechanics, or General Relativity, such as the differential equations for black hole perturbations Eq. (3) (where we can restore the first derivative if the standard radial coordinate is used instead of tortoise coordinates). Here we present a brief review concerning the AIM and discuss some implementation details of such a method. The AIM is based upon the following theorem:

**Theorem 1** *Let  $\lambda_0$  and  $s_0$  be functions of the variable  $x \in (a, b)$  that are  $C_\infty$  on the same interval. The differential equation (41) has a general solution of the form*

$$y(x) = \exp\left(-\int \alpha dt\right) \times \left[ C_2 + C_1 \int^x \exp\left(\int^t (\lambda_0(\tau) + 2\alpha(\tau))d\tau\right) dt \right] \tag{42}$$

if for some  $n > 0$  the condition

$$\alpha \equiv \frac{s_n}{\lambda_n} = \frac{s_{n-1}}{\lambda_{n-1}} \tag{43}$$

or equivalently

$$\delta \equiv s_n \lambda_{n-1} - \lambda_n s_{n-1} = 0 \tag{44}$$

is satisfied, where

$$\lambda_k(x) \equiv \lambda'_{k-1}(x) + s_{k-1}(x) + \lambda_0(x)\lambda_{k-1}(x) \tag{45}$$

$$s_k(x) \equiv s'_{k-1}(x) + s_0\lambda_{k-1}(x) \tag{46}$$

with  $k$  being a integer that ranges from 1 to  $n$ .

From now on, we shall refer to the condition expressed by Eq. (44) as the *AIM quantization condition*. Provided that Theo. 1 is satisfied we can find both the eigenvalues and eigenvectors of the second order ODE using, respectively, Eqs. (44) and (42). More specifically, the quasinormal modes of one perturbed black hole will be the complex frequency values  $\omega$  that satisfy Eq. (44) for any value of  $x$ .

Despite being quite general, the method presents a computational difficulty hidden in Eqs. (45) and (46): Not only the definition of the  $n$ -th coefficients are coupled and recursive they also involve the derivatives of previous entries. In practice this means that to compute the quantization condition, Eq. (44), using  $n$  iterations we end up computing the  $n$ -th derivatives of  $\lambda_0$  and  $s_0$  multiple times. Depending on the size of the original functions, the size and complexity of each coefficient can quickly spiral out of control. To address these issues, Cho et. al. have proposed in Ref. [43] to instead of computing these coefficients directly, use a Taylor expansion of both  $\lambda$  and  $s$  around a point  $\xi$  where the AIM is

to be performed (we remind the reader that the results are independent of the choice of  $\xi$ ), that is,

$$\lambda_n(\xi) = \sum_{i=0}^{\infty} c_n^i (x - \xi)^i, \tag{47}$$

$$s_n(\xi) = \sum_{i=0}^{\infty} d_n^i (x - \xi)^i, \tag{48}$$

where  $c_n^i$  and  $d_n^i$  are the Taylor coefficients of the expansions of  $\lambda_n$  and  $s_n$  around  $\xi$ , respectively. By plugging Eqs. (47) and (48) into Eqs. (45) and (46) one gets

$$c_n^i = (i + 1)c_{n-1}^{i+1} + d_{n-1}^i + \sum_{k=0}^i c_0^k c_{n-1}^{i-k}, \tag{49}$$

$$d_n^i = (i + 1)d_{n-1}^{i+1} + \sum_{k=0}^i d_0^k c_{n-1}^{i-k}. \tag{50}$$

Finally, using Eqs. (49) and (50) the quantization condition, Eq. (44), becomes

$$\delta \equiv d_n^0 c_{n-1}^0 - d_{n-1}^0 c_n^0 = 0. \tag{51}$$

In order to better visualize and understand the improved algorithm, it is useful to arrange the  $c_n^i$  (or  $d_n^i$ ) coefficients as elements  $c_{i,n}$  (or  $d_{i,n}$ ) of a matrix  $C$  (or  $D$ ), where the index  $i$  indicates the matrix row and the index  $n$  represents the matrix column, i.e.,

$$C = \begin{pmatrix} c_{0,0} & c_{0,1} & \cdots & c_{0,n-1} & c_{0,n} \\ c_{1,0} & c_{1,1} & \cdots & c_{1,n-1} & c_{1,n} \\ \vdots & \vdots & \ddots & \vdots & \vdots \\ c_{i,0} & c_{i,1} & \cdots & c_{i,n-1} & c_{i,n} \end{pmatrix}.$$

Notice that, when using Eq. (51), only the last and the before last top elements of the matrix (from left to right) are actually required, i.e., only the elements  $c_{0,n-1}$  and  $c_{0,n}$  are necessary. Note also that, by using Eqs. (49) and (50), to compute an element in row  $i$  and column  $n$ , one needs to have previously computed the column  $n - 1$  up to at least row  $i + 1$ . In practice this means that the matrix  $C$  “grows diagonally” and in order to compute  $n$  columns, one needs at least  $i = n$  rows. This formulation motivates us to view Eqs. (49) and (50) not as recursion relations, but as recipes for iteration, i.e., given the first column of the matrix  $C$ , one can use Eqs. (49) and (50) rewritten as

$$c_{n+1}^i = (i + 1)c_n^{i+1} + d_n^i + \sum_{k=0}^i c_0^k c_n^{i-k}, \tag{52}$$

$$d_{n+1}^i = (i + 1)d_n^{i+1} + \sum_{k=0}^i d_0^k c_n^{i-k}, \tag{53}$$

to compute the next column of the matrix.

With this insight, we can now devise an algorithm that performs  $n$  iterations of the AIM. Remember that if  $n$  iterations are to be performed, one needs at least  $i = n$  rows of coefficients and thus we shall truncate the Taylor expansions at  $i = n$ . The algorithm steps are the following:

1. Construct two arrays of size  $n$  where the  $i$ -th element is  $c_0^i$  (or  $d_0^i$ ) where  $i$  ranges from zero to  $n$ . We shall call these `icda` (initial  $c$  data array) and `idda` (initial  $d$  data array).
2. Construct two arrays of size  $n$  to contain the current column of  $c$  (or  $d$ ) indexes. We shall call these `ccda` (current  $c$  data array) and `cdca` (current  $d$  data array)
3. Construct two arrays of size  $n$  to contain the previous column of  $c$  (or  $d$ ) indexes. We shall call these `pcda` (previous  $c$  data array) and `pdda` (previous  $d$  data array).
4. Initialize `ccda` with data from `icda` and `cdca` with data from `idda`.
5. Perform  $n$  AIM steps using the evolution Eqs. (52) and (53). That is, repeat the following  $n$  times:
  - (a) Copy the content from `ccda` into `pcda`
  - (b) Copy the content from `cdca` into `pdda`
  - (c) Rewrite each element of `ccda` and `cdca` using Eqs. (52) and (53), respectively.
6. After  $n$  iterations, the current and previous data array contain the sought coefficients. Apply the quantization condition, Eq. (51), using the first indexes of each array (as they represent the  $i = 0$  coefficients). Explicitly, perform `cdca[1]*pcda[1] - pdda[1]*ccda[1]`<sup>1</sup>.
7. Finding the roots of the resulting expression from the last step yields the eigenvalues of the ODE (in the context of this work, the quasinormal modes).

This implementation is realized in the Julia [55] package called `QuasinormalModes.jl` [56]. The implementation makes use of an additional buffer array for each coefficient family in order to allow for thread-based parallelization to take place during the main AIM loop. All AIM numerical results from this work were obtained with the aforementioned package.

## 5 Numerical results for the QN frequencies

### 5.1 Spin 0 QN frequencies

Our numerical results for the quasinormal frequencies of the spin 0 perturbation field are displayed in Table 1. The first two

columns show the data from the pseudo-spectral method with different numbers of interpolating polynomials, the third column shows the results from the AIM method, while the fourth and fifth columns are reproduction of the results from Refs. [41,42], respectively. Notice that in Refs. [41,42] the WKB method was used to calculate the quasinormal frequencies. As can be seen, the pseudo-spectral method I (calculated with 60 polynomials) and pseudo-spectral method II (calculated with 40 polynomials) provide results, which are practically the same as those provided by the AIM, within six decimal places of precision. The numerical methods employed here provide more accurate results than those obtained by using the WKB approximation and allows us to calculate additional frequencies for spin 0 fields not reported previously in the literature.

### 5.2 Spin 1 QN frequencies

Our numerical results for the quasinormal frequencies for spin 1 fields are displayed in Table 2 compared against the results of Refs. [41,42], where the WKB method was employed. The first two columns show the data from the pseudo-spectral method with different numbers of interpolating polynomials, the third column shows the results from the AIM method, while the fourth and fifth columns are reproductions of the results from Refs. [41,42], respectively. As can be seen from the table, the pseudo-spectral method I (calculated with 60 polynomials) and pseudo-spectral method II (calculated with 40 polynomials) provide results that are practically identical to those provided by the AIM. The numerical methods we are working with provide more accurate results than those obtained by using the WKB approximation and allow us to present additional frequencies for spin 1 fields not reported previously in the literature.

### 5.3 Spin 2 QN frequencies

Our numerical results for the quasinormal frequencies of the spin 2 perturbation field are displayed in Table 3 compared against the results of Refs. [41,42], where the WKB method was employed. The first two columns show the data from the pseudo-spectral method with different numbers of interpolating polynomials, the third column shows the results from the AIM method, while the fourth and fifth columns are reproductions of the results from Refs. [41,42], respectively. As seen from the table, the pseudo-spectral method I and pseudo-spectral method II provide results that are practically equal to those provided by the AIM. The numerical results we are working with provide more accurate results than those obtained by employing the WKB approximation. It is worth mentioning that, in this case, we obtain additional solutions to the eigenvalue problem which does not represent gravi-

<sup>1</sup> Given that Julia uses 1 based array indexes, we are also using 1 based arrays for the algorithmic description. This means `cdca[1]` refers to the first element of the `cdca` array and so on so forth.

**Table 1** Quasinormal frequencies of the spin 0 perturbations normalized by the mass ( $M\omega$ ) compared against the results of Refs. [41,42]

$l$	$n$	Pseudo-spectralII (60 polynomials)	Pseudo-spectralII (40 polynomials)	AIM100 iterations	Ref. [41]	Ref. [42]
0	0	$\pm 0.110455 - 0.104896i$	$\pm 0.110455 - 0.104896i$	$\pm 0.110455 - 0.104896i$	$0.1046 - 0.1152i$	$\pm 0.1105 - 0.1008i$
1	0	$\pm 0.292936 - 0.097660i$	$\pm 0.292936 - 0.097660i$	$\pm 0.292936 - 0.097660i$	$0.2911 - 0.0980i$	$\pm 0.2929 - 0.0978i$
	1	$\pm 0.264449 - 0.306257i$	$\pm 0.264449 - 0.306257i$	$\pm 0.264449 - 0.306257i$	–	$\pm 0.2645 - 0.3065i$
2	0	$\pm 0.483644 - 0.096759i$	$\pm 0.483644 - 0.096759i$	$\pm 0.483644 - 0.096759i$	$0.4832 - 0.0968i$	$\pm 0.4836 - 0.0968i$
	1	$\pm 0.463851 - 0.295604i$	$\pm 0.463851 - 0.295604i$	$\pm 0.463851 - 0.295604i$	$0.4632 - 0.2958i$	$\pm 0.4638 - 0.2956i$
	2	$\pm 0.430544 - 0.508558i$	$\pm 0.430544 - 0.508558i$	$\pm 0.430544 - 0.508558i$	–	$\pm 0.4304 - 0.5087i$
3	0	$\pm 0.675366 - 0.096500i$	$\pm 0.675366 - 0.096500i$	$\pm 0.675366 - 0.096500i$	$0.6752 - 0.0965i$	–
	1	$\pm 0.660671 - 0.292285i$	$\pm 0.660671 - 0.292285i$	$\pm 0.660671 - 0.292285i$	$0.6604 - 0.2923i$	–
	2	$\pm 0.633626 - 0.496008i$	$\pm 0.633626 - 0.496008i$	$\pm 0.633626 - 0.496008i$	$0.6348 - 0.4941i$	–
	3	$\pm 0.598773 - 0.711221i$	$\pm 0.598773 - 0.711221i$	$\pm 0.598773 - 0.711221i$	–	–
4	0	$\pm 0.867416 - 0.096392i$	$\pm 0.867416 - 0.096392i$	$\pm 0.867416 - 0.096392i$	$0.8673 - 0.0964i$	–
	1	$\pm 0.855808 - 0.290876i$	$\pm 0.855808 - 0.290876i$	$\pm 0.855808 - 0.290876i$	$0.8557 - 0.2909i$	–
	2	$\pm 0.833692 - 0.490325i$	$\pm 0.833692 - 0.490325i$	$\pm 0.833692 - 0.490325i$	$0.8345 - 0.4895i$	–
	3	$\pm 0.803288 - 0.697482i$	$\pm 0.803288 - 0.697482i$	$\pm 0.803288 - 0.697482i$	$0.8064 - 0.6926i$	–
	4	$\pm 0.767733 - 0.914019i$	$\pm 0.767733 - 0.914019i$	$\pm 0.767733 - 0.914019i$	–	–

**Table 2** Quasinormal frequencies of the spin 1 perturbations normalized by the mass ( $M\omega$ ) compared against the results of Refs. [41,42]

$l$	$n$	Pseudo-spectralII (60 polynomials)	Pseudo-spectralII (40 polynomials)	AIM100 iterations	Ref. [41]	Ref. [42]
1	0	$\pm 0.248263 - 0.092488i$	$\pm 0.248263 - 0.092488i$	$\pm 0.248263 - 0.092488i$	$0.2459 - 0.0931i$	$\pm 0.2482 - 0.0926i$
	1	$\pm 0.214515 - 0.293668i$	$\pm 0.214515 - 0.293667i$	$\pm 0.214515 - 0.293668i$	–	$\pm 0.2143 - 0.2941i$
2	0	$\pm 0.457596 - 0.095004i$	$\pm 0.457595 - 0.095004i$	$\pm 0.457596 - 0.095004i$	$0.4571 - 0.0951i$	$\pm 0.4576 - 0.0950i$
	1	$\pm 0.436542 - 0.290710i$	$\pm 0.436542 - 0.290710i$	$\pm 0.436542 - 0.290710i$	$0.4358 - 0.2910i$	$\pm 0.4365 - 0.2907i$
	2	$\pm 0.401187 - 0.501587i$	$\pm 0.401187 - 0.501587i$	$\pm 0.401187 - 0.501587i$	–	$\pm 0.4009 - 0.5017i$
3	0	$\pm 0.656899 - 0.095616i$	$\pm 0.656899 - 0.095616i$	$\pm 0.656899 - 0.095616i$	$0.6567 - 0.0956i$	$\pm 0.6569 - 0.0956i$
	1	$\pm 0.641737 - 0.289728i$	$\pm 0.641737 - 0.289728i$	$\pm 0.641737 - 0.289728i$	$0.6415 - 0.2898i$	$\pm 0.6417 - 0.2897i$
	2	$\pm 0.613832 - 0.492066i$	$\pm 0.613832 - 0.492066i$	$\pm 0.613832 - 0.492066i$	$0.6151 - 0.4901i$	$\pm 0.6138 - 0.4921i$
	3	$\pm 0.577919 - 0.706331i$	$\pm 0.577919 - 0.706331i$	$\pm 0.577919 - 0.706330i$	–	$\pm 0.5775 - 0.7065i$
4	0	$\pm 0.853095 - 0.095860i$	$\pm 0.853095 - 0.095860i$	$\pm 0.853095 - 0.095810i$	$0.8530 - 0.0959i$	–
	1	$\pm 0.841267 - 0.289315i$	$\pm 0.841267 - 0.289315i$	$\pm 0.841267 - 0.289315i$	$0.8411 - 0.2893i$	–
	2	$\pm 0.818728 - 0.487838i$	$\pm 0.818728 - 0.487838i$	$\pm 0.818728 - 0.487838i$	$0.8196 - 0.4870i$	–
	3	$\pm 0.787748 - 0.694242i$	$\pm 0.787748 - 0.694242i$	$\pm 0.787748 - 0.694242i$	$0.7909 - 0.6892i$	–
	4	$\pm 0.751549 - 0.910242i$	$\pm 0.751549 - 0.910242i$	$\pm 0.751549 - 0.910242i$	–	–

tational waves, see the discussion in Appendix B for more details on this point.

### 5.4 Spin 1/2 QN frequencies

Our numerical results for the quasinormal frequencies for spin 1/2 fields are displayed in Table 4 compared against results available in the literature. The first two columns show the data from the pseudo-spectral method with different numbers of interpolating polynomials, the third column shows the results from the AIM method, while the fourth and fifth columns are reproductions of the results from Refs. [40,41], respectively. As can be seen, the results obtained using the

pseudo-spectral I and II are in perfect agreement with the results obtained using the AIM within the decimal places considered. Note that the numerical methods we are working with provide more accurate results than the results reported in Refs. [40,41], where the authors employed the WKB approximation. Note that we also show additional frequencies not reported previously in the literature, for example for  $\ell = 1$  and  $n = 1$ .

It is worth pointing out that we also found purely imaginary frequencies, that arise when investigating the quasinormal modes in the limit of large  $\ell$ . Our numerical results are displayed in Table 5, where we show the first five purely imaginary frequencies. As it is seen from the table, the agree-

**Table 3** Quasinormal frequencies of spin 2 perturbations normalized by the mass ( $M\omega$ ) compared against the results of Refs. [41,42]

$l$	$n$	Pseudo-spectralII (60 polynomials)	Pseudo-spectralII (40 polynomials)	AIM100 iterations	Ref. [41]	Ref. [42]
2	0	$\pm 0.373672 - 0.088962i$	$\pm 0.373672 - 0.088962i$	$\pm 0.373672 - 0.088962i$	$0.3730 - 0.0891i$	$\pm 0.3736 - 0.0890i$
	1	$\pm 0.346711 - 0.273915i$	$\pm 0.346711 - 0.273915i$	$\pm 0.346711 - 0.273915i$	$0.3452 - 0.2746i$	$\pm 0.3463 - 0.2735i$
	2	$\pm 0.301053 - 0.478277i$	$\pm 0.301053 - 0.478277i$	$\pm 0.301053 - 0.478277i$	-	$\pm 0.2985 - 0.4776i$
3	0	$\pm 0.599443 - 0.092703i$	$\pm 0.599443 - 0.092703i$	$\pm 0.599443 - 0.092703i$	$0.5993 - 0.0927i$	$\pm 0.5994 - 0.0927i$
	1	$\pm 0.582644 - 0.281298i$	$\pm 0.582644 - 0.281298i$	$\pm 0.582644 - 0.281298i$	$0.5824 - 0.2814i$	$\pm 0.5826 - 0.2813i$
	2	$\pm 0.551685 - 0.479093i$	$\pm 0.551685 - 0.479093i$	$\pm 0.551685 - 0.479027i$	$0.5532 - 0.4767i$	$\pm 0.5516 - 0.4790i$
4	0	$\pm 0.809178 - 0.094164i$	$\pm 0.809178 - 0.094164i$	$\pm 0.809178 - 0.094164i$	$0.8091 - 0.0942i$	$\pm 0.8092 - 0.0942i$
	1	$\pm 0.796632 - 0.284334i$	$\pm 0.796632 - 0.284334i$	$\pm 0.796632 - 0.284334i$	$0.7965 - 0.2844i$	$\pm 0.7966 - 0.2843i$
	2	$\pm 0.772710 - 0.479908i$	$\pm 0.772710 - 0.479908i$	$\pm 0.772710 - 0.479908i$	$0.7736 - 0.4790i$	$\pm 0.7727 - 0.4799i$
	3	$\pm 0.739837 - 0.683924i$	$\pm 0.739837 - 0.683924i$	$\pm 0.739837 - 0.683924i$	$0.7433 - 0.6783i$	$\pm 0.7397 - 0.6839i$
4	$\pm 0.701516 - 0.898239i$	$\pm 0.701516 - 0.898239i$	$\pm 0.701516 - 0.898239i$	-	$\pm 0.7006 - 0.8985i$	

**Table 4** Quasinormal frequencies of the spin 1/2 perturbations normalized by the mass ( $M\omega$ ) compared against the results of Refs. [40,41]

$l$	$n$	Pseudo-spectralII (60 polynomials)	Pseudo-spectralII (40 polynomials)	AIM100 iterations	Ref. [41]	Ref. [40]
0	0	$\pm 0.182963 - 0.096982i$	$\pm 0.182963 - 0.096982i$	$\pm 0.182963 - 0.096824i$	-	-
1	0	$\pm 0.380037 - 0.096405i$	$\pm 0.380037 - 0.096405i$	$\pm 0.380037 - 0.096405i$	$0.3786 - 0.0965i$	$0.379 - 0.097i$
	1	$\pm 0.355833 - 0.297497i$	$\pm 0.355833 - 0.297497i$	$\pm 0.355833 - 0.297497i$	-	-
2	0	$\pm 0.574094 - 0.096305i$	$\pm 0.574094 - 0.096305i$	$\pm 0.574094 - 0.096305i$	$0.5737 - 0.0963i$	$0.574 - 0.096i$
	1	$\pm 0.557015 - 0.292715i$	$\pm 0.557015 - 0.292715i$	$\pm 0.557015 - 0.292715i$	$0.5562 - 0.2930i$	$0.556 - 0.293i$
	2	$\pm 0.526607 - 0.499695i$	$\pm 0.526607 - 0.499695i$	$\pm 0.526607 - 0.499695i$	-	-
3	0	$\pm 0.767355 - 0.096270i$	$\pm 0.767355 - 0.096270i$	$\pm 0.767355 - 0.096270i$	$0.7672 - 0.0963i$	$0.767 - 0.096i$
	1	$\pm 0.754300 - 0.290968i$	$\pm 0.754300 - 0.290968i$	$\pm 0.754300 - 0.290968i$	$0.7540 - 0.2910i$	$0.754 - 0.291i$
	2	$\pm 0.729770 - 0.491910i$	$\pm 0.729770 - 0.491910i$	$\pm 0.729770 - 0.491910i$	$0.7304 - 0.4909i$	$0.730 - 0.491i$
4	0	$\pm 0.960293 - 0.096254i$	$\pm 0.960293 - 0.096254i$	$\pm 0.960293 - 0.096254i$	$0.9602 - 0.0963i$	$0.960 - 0.096i$
	1	$\pm 0.949759 - 0.290148i$	$\pm 0.949759 - 0.290148i$	$\pm 0.949759 - 0.290148i$	$0.9496 - 0.2902i$	$0.950 - 0.290i$
	2	$\pm 0.929494 - 0.488116i$	$\pm 0.929494 - 0.488116i$	$\pm 0.929494 - 0.488116i$	$0.9300 - 0.4876i$	$0.930 - 0.488i$
	3	$\pm 0.901129 - 0.692520i$	$\pm 0.901129 - 0.692520i$	$\pm 0.901129 - 0.692520i$	$0.9036 - 0.6892i$	$0.904 - 0.689i$
4	$\pm 0.867043 - 0.905047i$	$\pm 0.867008 - 0.905066i$	$\pm 0.867043 - 0.905047i$	-	-	

**Table 5** Purely imaginary frequencies for spin 1/2 perturbations normalized by the mass ( $M\omega$ ). The numerical values of such frequencies are exactly the same as for the purely imaginary frequencies arising in the QNM of spin 3/2 perturbations

Pseudo-spectralII (60 polynomials)	(60Pseudo-spectralII polynomials)	(40AIM100 iterations)
$-0.250000i$	$-0.250000i$	$-0.250000i$
$-0.500000i$	$-0.500000i$	$-0.500000i$
$-0.750000i$	$-0.750000i$	$-0.750000i$
$-1.000000i$	$-1.000000i$	$-1.000031i$
$-1.2499998i$	$-1.250000i$	$-1.246550i$

ment between the numerical methods is perfect for low overtones but it gets worse for higher overtones. It is worth men-

tioning that these results are in perfect agreement with the analytic solution,  $M\omega = -in/4$ ,  $n \rightarrow \infty$ , obtained in Refs. [57,58], see also references therein.

### 5.5 Spin 3/2 QN frequencies

Our numerical results for the quasinormal frequencies for spin 3/2 field are displayed in Table 6 compared against results available in the literature. The first two columns show the data from the pseudo-spectral method with different numbers of interpolating polynomials, the third column shows the results from the AIM method, while the fourth and fifth columns are reproductions of the results from Refs. [41,49], respectively. As can be seen, the results obtained using the pseudo-spectral I and II are in perfect agreement with the

**Table 6** Quasinormal frequencies of spin 3/2 perturbations normalized by the mass ( $M\omega$ ) compared against the results of Refs. [41, 49]

$l$	$n$	Pseudo-spectralII (60 polynomials)	Pseudo-spectralII (40 polynomials)	AIM100 iterations	Ref. [41]	Ref. [49]
0	0	$\pm 0.311292 - 0.090087i$	$\pm 0.311292 - 0.090087i$	$\pm 0.311292 - 0.090087i$	–	$0.3112 - 0.0902i$
1	0	$\pm 0.530048 - 0.093751i$	$\pm 0.530048 - 0.093751i$	$\pm 0.530048 - 0.093751i$	–	$0.5300 - 0.0937i$
	1	$\pm 0.511392 - 0.285423i$	$\pm 0.511392 - 0.285423i$	$\pm 0.511392 - 0.285423i$	–	$0.5113 - 0.2854i$
2	0	$\pm 0.734750 - 0.094878i$	$\pm 0.734750 - 0.094878i$	$\pm 0.734750 - 0.094878i$	$\pm 0.7346 - 0.0949i$	$0.7347 - 0.0948i$
	1	$\pm 0.721047 - 0.286906i$	$\pm 0.721047 - 0.286906i$	$\pm 0.721047 - 0.286906i$	$\pm 0.7206 - 0.2870i$	$0.7210 - 0.2869i$
	2	$\pm 0.695287 - 0.485524i$	$\pm 0.695287 - 0.485524i$	$\pm 0.695287 - 0.485524i$	–	$0.6952 - 0.4855i$
3	0	$\pm 0.934364 - 0.095376i$	$\pm 0.934364 - 0.095376i$	$\pm 0.934364 - 0.095376i$	$\pm 0.9343 - 0.0954i$	$0.9343 - 0.0953i$
	1	$\pm 0.923502 - 0.287560i$	$\pm 0.923502 - 0.287560i$	$\pm 0.923502 - 0.287560i$	$\pm 0.9233 - 0.2876i$	$0.9235 - 0.2875i$
	2	$\pm 0.902599 - 0.483957i$	$\pm 0.902599 - 0.483957i$	$\pm 0.902599 - 0.483957i$	$\pm 0.9031 - 0.4835i$	$0.9025 - 0.4839i$
	3	$\pm 0.873342 - 0.687024i$	$\pm 0.873343 - 0.687024i$	$\pm 0.873342 - 0.687024i$	–	$0.8732 - 0.6870i$
4	0	$\pm 1.131530 - 0.095640i$	$\pm 1.131530 - 0.095640i$	$\pm 1.131530 - 0.095640i$	$\pm 1.1315 - 0.0956i$	$1.1315 - 0.0956i$
	1	$\pm 1.122523 - 0.287908i$	$\pm 1.122523 - 0.287908i$	$\pm 1.122523 - 0.287908i$	$\pm 1.1224 - 0.2879i$	$1.1225 - 0.2879i$
	2	$\pm 1.104976 - 0.483096i$	$\pm 1.104976 - 0.483096i$	$\pm 1.104976 - 0.483096i$	$\pm 1.1053 - 0.4828i$	$1.1049 - 0.4830i$
	3	$\pm 1.079852 - 0.683000i$	$\pm 1.079852 - 0.683000i$	$\pm 1.079852 - 0.683000i$	$\pm 1.0817 - 0.6812i$	$1.0798 - 0.6829i$
	4	$\pm 1.048599 - 0.889113i$	$\pm 1.048596 - 0.889115i$	$\pm 1.048599 - 0.889113i$	–	$1.0484 - 0.8890i$

**Table 7** Quasinormal frequencies of spin 5/2 perturbations normalized by the mass ( $M\omega$ )

$l$	$n$	Pseudo-spectralII (60 polynomials)	Pseudo-spectralII (40 polynomials)	AIM100 iterations
0	0	$\pm 0.462727 - 0.092578i$	$\pm 0.462727 - 0.092578i$	$0.462727 - 0.092577i$
1	0	$\pm 0.687103 - 0.094566i$	$\pm 0.687103 - 0.094566i$	$0.687103 - 0.094566i$
	1	$\pm 0.670542 - 0.285767i$	$\pm 0.670542 - 0.285767i$	$0.670542 - 0.285767i$
2	0	$\pm 0.897345 - 0.095309i$	$\pm 0.897345 - 0.095309i$	$0.897345 - 0.095309i$
	1	$\pm 0.884980 - 0.287266i$	$\pm 0.884980 - 0.287266i$	$0.884980 - 0.287266i$
	2	$\pm 0.861109 - 0.483113i$	$\pm 0.861109 - 0.483113i$	$0.861109 - 0.483113i$
3	0	$\pm 1.101190 - 0.095648i$	$\pm 1.101190 - 0.095648i$	$1.101190 - 0.095648i$
	1	$\pm 1.091300 - 0.287886i$	$\pm 1.091300 - 0.287886i$	$1.091300 - 0.287886i$
	2	$\pm 1.071999 - 0.482895i$	$\pm 1.071999 - 0.482895i$	$1.071999 - 0.482895i$
	3	$\pm 1.044272 - 0.682307i$	$\pm 1.044272 - 0.682307i$	$1.044272 - 0.682307i$
4	0	$\pm 1.301587 - 0.095829i$	$\pm 1.301587 - 0.095829i$	$1.301587 - 0.095829i$
	1	$\pm 1.293328 - 0.288184i$	$\pm 1.293328 - 0.288184i$	$1.293328 - 0.288184i$
	2	$\pm 1.277107 - 0.482604i$	$\pm 1.277107 - 0.482604i$	$1.277107 - 0.482604i$
	3	$\pm 1.253526 - 0.680366i$	$\pm 1.253526 - 0.680366i$	$1.253526 - 0.680366i$
	4	$\pm 1.223513 - 0.882554i$	$\pm 1.223512 - 0.882553i$	$1.223513 - 0.882554i$

results obtained using the AIM. We also realized that these results are in very good agreement with the results reported in Ref. [49], where the authors also employed the AIM, and with the results from Ref. [41], where the authors employed the WKB approximation.

As in the spin 1/2 field perturbations, we also find purely imaginary frequencies for the spin 3/2 field. The numerical results are displayed in Table 5 for the three routines we are working with. Such frequencies arise when investigating the quasinormal modes in the limit of large  $\ell$ . Notice that these results are also in agreement with the analytic solutions obtained in Refs. [57, 58]. It is worth pointing out that

the numerical values of these purely imaginary frequencies are the same for spin 1/2 and 3/2 fields. We do not have an explanation for this fact, maybe it is just a coincidence. Notice also that these frequencies can be written as fractions, multiples of 1/4, i.e., 1/4, 2/4, 3/4, 4/4,  $\sim 5/4, \dots$

### 5.6 Spin 5/2 QN frequencies

Our numerical results for the quasinormal frequencies for spin 5/2 fields are displayed in Table 7. As can be seen, the results obtained by using the pseudo-spectral I and II are in perfect agreement with the results obtained using the AIM

**Table 8** Purely imaginary frequencies of spin 5/2 perturbations normalized by the mass ( $M\omega$ )

Pseudo-spectralII polynomials)	(60Pseudo-spectralII polynomials)	(40AIM100 iterations polynomials)
-0.125000i	-0.125000i	-0.125000i
-0.375602i	-0.375602i	-0.378659i
-0.626877i	-0.626877i	-0.623931i
-0.878946i	-0.878948i	-0.907374i

within the decimal places considered. It is worth mentioning that we present here the quasinormal frequencies for spin 5/2 perturbation fields for the very first time.

In turn, we also found purely imaginary frequencies. Our numerical results are displayed in Table 8. It turns out that these results satisfy the sequence  $1/8, \sim 3/8, \sim 5/8, \sim 7/8, \dots$ , in general,

$$M\omega = -i \frac{(2n + 1)}{8}, \quad n = 0, 1, 2, 3, \dots \tag{54}$$

As it happens in the cases of spin 1/2 and 3/2 perturbations, these frequencies arise when investigating the frequencies in the limit of large  $\ell$ . As can be seen, the discrepancy between both methods increases as the imaginary frequency gets negative.

### 6 QNMs for $\ell \gg 1$ and $n \gg 1$

It is also interesting to calculate the quasinormal frequencies in the limit of large  $\ell$ , where analytic solutions are available in the literature to compare with. The analytic solutions were obtained in Ref. [59], such that the real and imaginary parts of the frequencies are given by

$$\begin{aligned} M\omega_{\text{Re}} &= \frac{1}{3\sqrt{3}} \left( \ell + \frac{1}{2} \right), \\ M\omega_{\text{Im}} &= -\frac{1}{3\sqrt{3}} \left( n + \frac{1}{2} \right). \end{aligned} \tag{55}$$

Before comparing our numerical results against the analytic solutions, it is worth mentioning that these analytic solutions were obtained for integer spin perturbations. We do not expect that these results can be applied for semi-integer field perturbations, in principle.

Let us now compare our numerical results against the analytic solutions (55). Our numerical results for  $s = 0$  field are displayed in Figs. 1 and 2, as a function of  $\ell$  and  $n$ , respectively. As can be seen, the real part as a function of  $\ell$  fits well the analytic result (55). Meanwhile, the imaginary part of the frequency as a function of  $n$  also fits well the analytic solution.

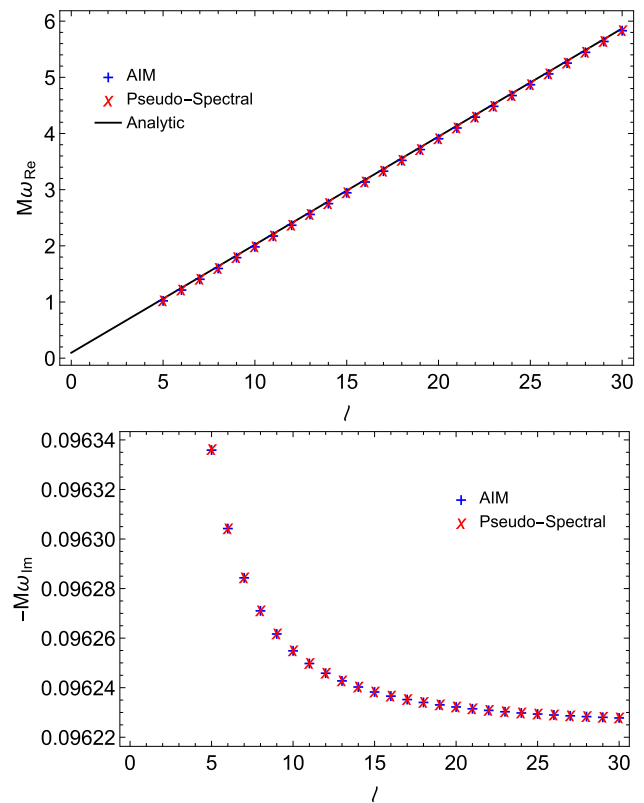


**Fig. 1** The real (top panel) and imaginary (bottom panel) parts of the frequency as a function of  $\ell$  for the scalar  $s = 0$  field in the case  $n = 0$ , the fundamental mode. The crosses (+) represent the AIM results, the exes (x) indicate the pseudo-spectral, while the solid black line in the top panel is the plot of the function  $M\omega_{\text{Re}}$  given in Eq. (55)

It is worth pointing out that the numerical results obtained using the pseudo-spectral and AIM are in agreement, as seen in these figures. To observe the numerical difference we plotted the difference of the frequencies  $|M\omega_{\text{Re}}^{\text{AIM}} - M\omega_{\text{Re}}^{\text{PS}}|$  and  $|M\omega_{\text{Im}}^{\text{AIM}} - M\omega_{\text{Im}}^{\text{PS}}|$  in logarithmic scale and displayed the results in Fig. 3. It is seen that the difference between the numerical results is very small and slightly increases with the increase of  $n$ .

In turn, our numerical results for the spin 1/2 perturbation field are displayed in Fig. 4. As can be seen, the numerical and analytic results are in agreement. This means that the analytic results are also valid for perturbations for spin 1/2.

### 7 Discussion and conclusion

We have calculated the quasinormal frequencies for spin 0, 1/2, 1, 3/2, 2, and 5/2 fields on the Schwarzschild black hole in asymptotically flat space-time. We have employed the pseudo-spectral and AIM methods. The main difference between these methods lies in the way they solve the eigenvalue problem. While the pseudo-spectral method expands

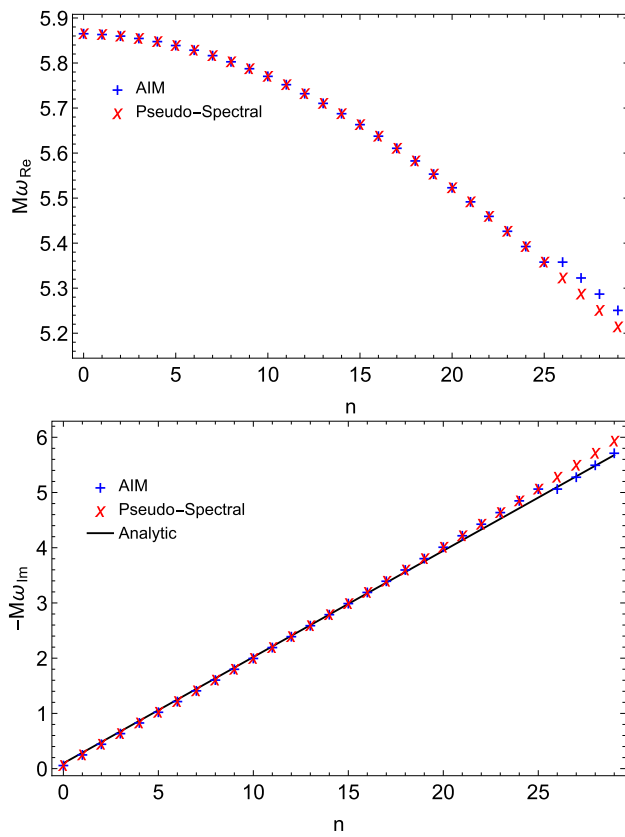


**Fig. 2** The real (top panel) and imaginary (bottom panel) parts of the frequency as a function of  $n$  for the spin  $s = 0$  field with  $\ell = 30$ . The crosses (+) represent the AIM results, the exes (x) indicate the pseudo-spectral, while the solid black line in the bottom panel is the plot of the function  $M\omega_{Im}$  given in Eq. (55)

the solution on a base of cardinal functions, the AIM calculates the roots of a characteristic polynomial. In doing so, the results obtained for a spin-zero field applying the pseudo-spectral method are in good agreement with the results obtained by employing the AIM and also in good agreement with literature values.

We displayed results with six decimal places in Tables 1, 2 and 3. The results show that both methods are in agreement at least up to the sixth decimal place. We point out that the quasinormal frequencies obtained for spin 0, 1, and 2 fields do not bring any additional information to what we know from the literature. In turn, for spin 1/2 and 3/2 fields, our results obtained for both methods are in agreement, these results are also in agreement with results available in the literature. For these fields, we have obtained additional frequencies which are purely imaginary, see Table 5. We also calculated the quasinormal frequencies for a spin 5/2 field, which are displayed in Table 7. We have observed that the pseudo-spectral method and the AIM show good agreement. Additional frequencies, which are purely imaginary, were also obtained and displayed in Table 8. Hence, the pseudo-spectral method calculated a set of quasinormal frequencies, while the AIM

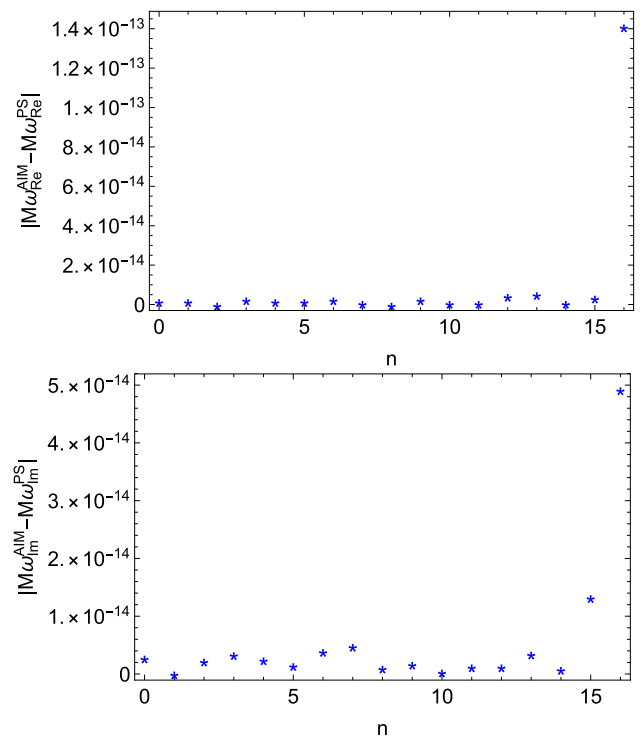


**Fig. 3** The figure shows the difference between the frequencies obtained by means of the AIM and the ones obtained from the pseudo-spectral method, in logarithmic scale, as a function of  $n$  for the spin  $s = 0$  perturbation field. The top panel is for the real part of the frequency, while the bottom panel is for the imaginary part of the frequency

used a guess to start looking for solutions. Our main conclusion is that both methods complemented each other in the task of calculating the QNM frequencies.

Additional comments concerning the numerical analysis may be of interest. The use of 60 polynomials for the pseudo-spectral method I and 40 polynomials for the pseudo-spectral method II are the minima necessary to reach the precision one desires in the calculation, say 30 decimal places in such a case. An additional issue concerning the pseudo-spectral method is related to the reason why such a method does not yield, for instance, the 30 expected eigen-frequencies for  $\ell = 30$ . We tried increasing the number of polynomials but, with fixed precision, we were unable to go beyond 16 solutions. We realized that by increasing the number of polynomials and the precision we were able to reach 30 eigen-frequencies. Similar difficulties are also present in the AIM: For certain problems (those with more simple ODE coefficients such as the quantum harmonic oscillator), the method furnishes the complete spectra of the ODE without the need for fine-tuning or arbitrary precision. For black hole problems, however, one can easily find 2 or 3 overtones of a mode without modifying the method’s parameters. Further overtones may or may not be found by tuning  $x_0$ , as this value affects the speed at which the method converges. At the time of writing this paper, it is not yet clear whether this

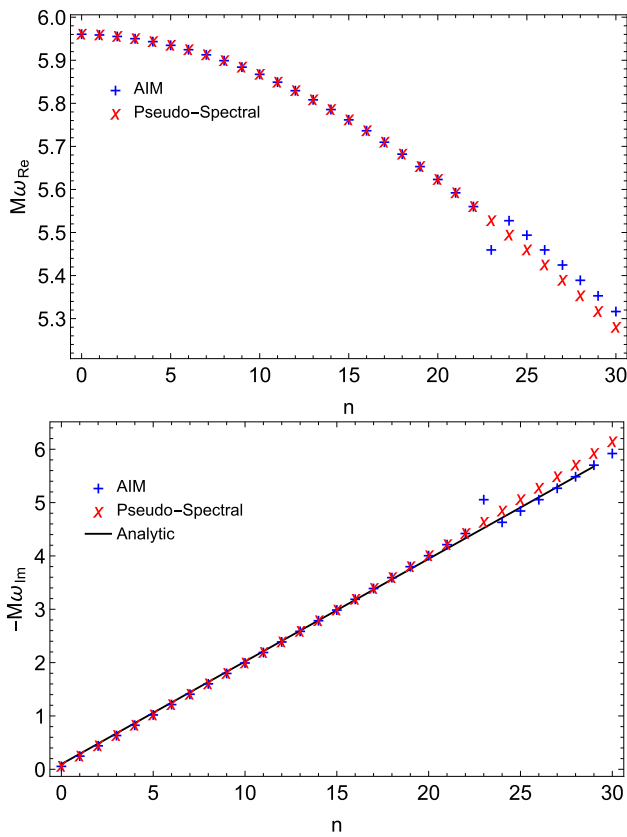


**Fig. 4** The figure shows the real (top panel) and imaginary (bottom panel) parts of the frequency as a function of  $n$  for the spin  $s = 1/2$  field in the case  $\ell = 30$ . The crosses (+) represent the AIM results, the exes (x) indicate the pseudo-spectral, while the solid black line in the bottom panel is the plot of the function  $M\omega_{Im}$  given in Eq. (55)

difficulty comes from the nature of the method itself or the implementation used in this work (where ODE coefficients are expanded using a Taylor series around  $x_0$ ), but we believe that such questions might be answered soon in the light of new works investigating the AIM’s applicability conditions such as [60]

In the next stage of the present work, we shall address the problem of calculating QNMs for massive test fields, extending the analysis to other black hole spacetimes such as the Reissner–Nordström, Kerr, and the Kerr–Newman black holes, as well as considering the contribution of the cosmological constant.

**Acknowledgements** We would like to acknowledge Alex S. Miranda for useful discussions along the development of this work. L. T. S. and A. D. D. M. are partly funded by Coordenação de Aperfeiçoamento de Pessoal de Nível Superior (CAPES), Brazil, Finance Code 001. V. T. Z. thanks financial support from Conselho Nacional de Desenvolvimento Científico e Tecnológico (CNPq), Brazil, Grant No. 309609/2018-6, and from CAPES, Brazil, Grant No. 88887.310351/2018-00.

**Data Availability Statement** This manuscript has no associated data or the data will not be deposited. [Authors’ comment: All data generated and analyzed during this study are included in this published article.]

**Open Access** This article is licensed under a Creative Commons Attribution 4.0 International License, which permits use, sharing, adaptation, distribution and reproduction in any medium or format, as long as you give appropriate credit to the original author(s) and the source, provide a link to the Creative Commons licence, and indicate if changes were made. The images or other third party material in this article are included in the article’s Creative Commons licence, unless indicated otherwise in a credit line to the material. If material is not included in the article’s Creative Commons licence and your intended use is not permitted by statutory regulation or exceeds the permitted use, you will need to obtain permission directly from the copyright holder. To view a copy of this licence, visit <http://creativecommons.org/licenses/by/4.0/>.

Funded by SCOAP<sup>3</sup>. SCOAP<sup>3</sup> supports the goals of the International Year of Basic Sciences for Sustainable Development.

### Appendix A: Fundamental equations for the spin 5/2 perturbations

Here we present additional details of the spin 5/2 field. First, we write the effective potential  $V_{5/2}(u)$  that appears in the Schrödinger-like equation when written in terms of the variable  $u = 1/r$ . It assumes the form

$$\begin{aligned}
 V_{5/2} = \frac{u^2 f}{4S(u)} & \left\{ 4 \left[ 75L_2 (23 + 3L_3) u + 9L_2^3 u^6 \right. \right. \\
 & + L_2^2 \left[ 25L_4 - 9u^7 (9 + L_3 \{3 + u^2 - 3u\} \right. \\
 & \left. \left. + u \{3 + 6u^2 - 13u\} \right) \right] - 450u^2 [2u - (3 + \ell)^2] \left. \right. \\
 & - 15u^2 f^{1/2} \left[ 2u \left( 35\sqrt{7 + L_3} - 221 + 4L_3^3 (u - 1) \right. \right. \\
 & + 3L_3^2 (\sqrt{7 + L_3} - 6u - 16) + 14u (5\sqrt{7 + L_3} - 98) \\
 & \left. \left. + L_3 (22\sqrt{7 + L_3} - 189 - 456u + 14u\sqrt{7 + L_3}) \right) \right. \\
 & \left. \left. + L_2 [12 - 20\sqrt{7 + L_3} + 9u^3 (33 + 46u) \right. \right. \\
 & \left. \left. + L_3 (141u^3 - 4\sqrt{7 + L_3}) \right] \right\}, \tag{A.1}
 \end{aligned}$$

where, to simplify the expressions, we introduced the notation

$$\begin{aligned}
 S(u) &= \left[ 5(L_2 + 6u) + 3L_2 u^3 f^{3/2}(u) \right]^2, \\
 L_1 &= 11 + \ell(6 + \ell), \\
 L_2 &= (1 + \ell)(5 + \ell), \\
 L_3 &= \ell(6 + \ell), \\
 L_4 &= (2 + \ell)(4 + \ell).
 \end{aligned}$$

Following the procedure explained in Sect. 2.2, we transform the Schrödinger-like equation into an equation suitable to apply the numerical methods we are working with. Moreover, to avoid square roots, we have used the variable  $\chi^2 = 1 - u$ , such that the final differential equation is

$$R(\chi)\phi_{5/2}(\chi) + Q(\chi)\phi'_{5/2}(\chi) + P(\chi)\phi''_{5/2}(\chi) = 0, \quad (\text{A.2})$$

where  $P(\chi)$ ,  $Q(\chi)$ , and  $R(\chi)$  are given by

$$\begin{aligned} R(\chi) = & \chi(1-\chi^2) \left[ 100L_2L_4 - 800L_2L_4(\chi^2-1) \right. \\ & + 60 \left[ 10(17+L_3) + L_2\chi(\sqrt{7+L_3}(5+L_3)-3) \right] \\ & \times (\chi^2-1)^2 + 15L_2\chi(305+133L_3)(\chi^2-1)^5 \\ & + 36L_2^2(10+3L_3)(\chi^2-1)^7 + 108L_2^2L_3(\chi^2-1)^8 \\ & + 36L_2^2(L_3-10)(\chi^2-1)^9 - 180L_2^2(\chi^2-1)^{10} \\ & + 18L_2(2(5+L_3)^2-305\chi)(\chi^2-1)^6 \\ & \left. - 60\chi \left[ 35\sqrt{7+L_3} - 636 \right. \right. \\ & \left. \left. + L_3(7\sqrt{7+L_3} - 208 + L_3(2L_3-7)) \right] (\chi^2-1)^4 \right] \\ & - 30\chi(1-\chi^2)^4 \left( 240 + \chi \left[ 35\sqrt{7+L_3} - 221 \right. \right. \\ & \left. \left. - L_3(189 - 22\sqrt{7+L_3} + L_3 \{ 48 - 3\sqrt{7+L_3} \right. \right. \right. \\ & \left. \left. \left. + 4L_3 \} \right) \right] \right) - 16\lambda\chi \left[ i + 4\lambda(2-3\chi^2 + \chi^4) \right] t(\chi), \\ Q(\chi) = & (\chi^2-1) \left[ 1 + \chi^2(\chi^2-2)(1-16i\lambda) - 8i\lambda \right] t(\chi), \\ P(\chi) = & \chi(\chi^2-1)^3 t(\chi), \end{aligned} \quad (\text{A.3})$$

where the auxiliary coefficient  $t(\chi)$  is given by  $t(\chi) = [30(\chi^2-1) + L_2(3\chi^9 - 9\chi^7 + 9\chi^5 - 3\chi^3 - 5)]^2$ .

### Appendix B: Further comments on the numerical QN frequencies

In this appendix we comment on additional details found when analyzing the quasinormal frequencies of the Schwarzschild black hole by employing the AIM and pseudo-spectral methods for integer spin perturbation fields  $s = 2$  and  $s = 1$ .

For completeness, we started our search for solutions to the eigenvalue problem for  $s = 2$  by setting  $\ell = 0$  in Eq. (17), we do not get any solution. Then, we set  $\ell = 1$  and we get the solutions  $M\omega_0 = \pm 0.110455 - 0.104896i$  and  $M\omega_1 = \pm 0.086158 - 0.348079i$ , corresponding to  $n = 0$  and  $n = 1$ , respectively. It is also interesting to point out that the solution for  $\ell = 1$  and  $n = 0$  arises in both methods employed in this work, while the solution for  $\ell = 1$  and  $n = 1$  arises in the asymptotic iteration method alone. As a consistency check, we solved the same problem by employing the Leaver continued fraction method [39] and obtained the same results as from the AIM. However, as investigated by Regge–Wheeler [61], and Zerilli [61] modes with  $\ell = 1$  represent an addition of angular momentum to the background

metric given by Eq. (1). Hence, such modes do not generate gravitational waves.

On the other hand, investigating the electromagnetic perturbation,  $s = 1$ , for  $\ell = 0$  we obtained

$$M\omega_n = -i \frac{(n+1)}{4}, \quad n = 0, 1, 2, \dots \quad (\text{B.4})$$

in both methods.

### References

1. H. Goldstein, *Classical Mechanics* (Addison-Wesley, Boston, 1980)
2. LIGO Scientific and Virgo Collaborations, B.P. Abbott et al., GW170817: observation of gravitational waves from a binary neutron star inspiral. *Phys. Rev. Lett.* **119**, 161101 (2017). [arXiv:1710.05832](https://arxiv.org/abs/1710.05832) [gr-qc]
3. LIGO Scientific and Virgo Collaborations, B.P. Abbott et al., Tests of general relativity with gw150914. *Phys. Rev. Lett.* **116** (2016)
4. E. Berti, V. Cardoso, A.O. Starinets, Quasinormal modes of black holes and black branes. *Class. Quantum Gravity* **26**, 163001 (2009)
5. R.A. Konoplya, A. Zhidenko, Quasinormal modes of black holes: from astrophysics to string theory. *Rev. Mod. Phys.* **83**, 793–836 (2011). [arXiv:1102.4014](https://arxiv.org/abs/1102.4014) [gr-qc]
6. J.W. York Jr., Dynamical origin of black hole radiance. *Phys. Rev. D* **28**, 2929 (1983)
7. V. Ferrari, B. Mashhoon, New approach to the quasinormal modes of a black hole. *Phys. Rev. D* **30**, 295–304 (1984)
8. E.W. Leaver, Spectral decomposition of the perturbation response of the Schwarzschild geometry. *Phys. Rev. D* **34**, 384–408 (1986)
9. H.-P. Nollert, B.G. Schmidt, Quasinormal modes of Schwarzschild black holes: defined and calculated via Laplace transformation. *Phys. Rev. D* **45**, 2617 (1992)
10. N. Andersson, S. Linnæus, Quasinormal modes of a Schwarzschild black hole: improved phase-integral treatment. *Phys. Rev. D* **46**, 4179 (1992)
11. H.-P. Nollert, Quasinormal modes of Schwarzschild black holes: the determination of quasinormal frequencies with very large imaginary parts. *Phys. Rev. D* **47**, 5253–5258 (1993)
12. K.D. Kokkotas, B.G. Schmidt, Quasinormal modes of stars and black holes. *Living Rev. Relativ.* **2**, 2 (1999). [arXiv:gr-qc/9909058](https://arxiv.org/abs/gr-qc/9909058)
13. G.T. Horowitz, V.E. Hubeny, Quasinormal modes of AdS black holes and the approach to thermal equilibrium. *Phys. Rev. D* **62**, 024027 (2000). [arXiv:hep-th/9909056](https://arxiv.org/abs/hep-th/9909056)
14. H.-P. Nollert, Topical Review: quasinormal modes: the characteristic ‘sound’ of black holes and neutron stars. *Class. Quantum Gravity* **16**, R159–R216 (1999)
15. V. Cardoso, J.P.S. Lemos, Scalar, electromagnetic and Weyl perturbations of BTZ black holes: quasinormal modes. *Phys. Rev. D* **63**, 124015 (2001). [arXiv:gr-qc/0101052](https://arxiv.org/abs/gr-qc/0101052)
16. V. Cardoso, J.P.S. Lemos, Quasinormal modes of Schwarzschild anti-de Sitter black holes: electromagnetic and gravitational perturbations. *Phys. Rev. D* **64**, 084017 (2001). [arXiv:gr-qc/0105103](https://arxiv.org/abs/gr-qc/0105103)
17. R.A. Konoplya, On quasinormal modes of small Schwarzschild-anti-de Sitter black hole. *Phys. Rev. D* **66**, 044009 (2002). [arXiv:hep-th/0205142](https://arxiv.org/abs/hep-th/0205142)
18. A.O. Starinets, Quasinormal modes of near extremal black branes. *Phys. Rev. D* **66**, 124013 (2002). [arXiv:hep-th/0207133](https://arxiv.org/abs/hep-th/0207133)
19. C.A. Clarkson, R.K. Barrett, Covariant perturbations of Schwarzschild black holes. *Class. Quantum Gravity* **20**, 3855–3884 (2003). [arXiv:gr-qc/0209051](https://arxiv.org/abs/gr-qc/0209051)

20. P.K. Kovtun, A.O. Starinets, Quasinormal modes and holography. *Phys. Rev. D* **72**, 086009 (2005). [arXiv:hep-th/0506184](#)
21. V. Cardoso, A.S. Miranda, E. Berti, H. Witek, V.T. Zanchin, Geodesic stability, Lyapunov exponents and quasinormal modes. *Phys. Rev. D* **79**, 064016 (2009). [arXiv:0812.1806](#) [hep-th]
22. A.S. Miranda, J. Morgan, V.T. Zanchin, Quasinormal modes of plane-symmetric black holes according to the AdS/CFT correspondence. *JHEP* **2008**, 030 (2008). [arXiv:0809.0297](#) [hep-th]
23. J. Morgan, V. Cardoso, A.S. Miranda, C. Molina, V.T. Zanchin, Gravitational quasinormal modes of AdS black branes in  $d$  space-time dimensions. *JHEP* **2009**, 117 (2009). [arXiv:0907.5011](#) [hep-th]
24. A.S. Miranda, C.A. Ballon Bayona, H. Boschi-Filho, N.R.F. Braga, Black-hole quasinormal modes and scalar glueballs in a finite-temperature AdS/QCD model. *JHEP* **2009**, 119 (2009). [arXiv:0909.1790](#) [hep-th]
25. L.A.H. Mamani, A.S. Miranda, H. Boschi-Filho, N.R.F. Braga, Vector meson quasinormal modes in a finite-temperature AdS/QCD model. *JHEP* **2014**, 1–26 (2014). [arXiv:1312.3815](#) [hep-th]
26. L.A.H. Mamani, J. Morgan, A.S. Miranda, V.T. Zanchin, From quasinormal modes of rotating black strings to hydrodynamics of a moving CFT plasma. *Phys. Rev. D* **98**, 026006 (2018). [arXiv:1804.01544](#) [gr-qc]
27. L.A.H. Mamani, A.S. Miranda, V.T. Zanchin, Melting of scalar mesons and black-hole quasinormal modes in a holographic QCD model. *Eur. Phys. J. C* **79**, 1–20 (2019). [arXiv:1809.03508](#) [hep-th]
28. L.A.H. Mamani, D. Hou, N.R.F. Braga, Melting of heavy vector mesons and quasinormal modes in a finite density plasma from holography. *Phys. Rev. D* **105**, 126020 (2022). [arXiv:2204.08068](#) [hep-ph]
29. Event Horizon Telescope Collaboration, K. Akiyama et al., First M87 event horizon telescope results. I. The shadow of the supermassive black hole. *Astrophys. J. Lett.* **875**, L1 (2019). [arXiv:1906.11238](#) [astro-ph.GA]
30. Event Horizon Telescope Collaboration, K. Akiyama et al., First M87 Event Horizon Telescope results. VI. The shadow and mass of the central black hole. *Astrophys. J. Lett.* **875**, L6 (2019). [arXiv:1906.11243](#) [astro-ph.GA]
31. V. Perlick, O.Y. Tsupko, G.S. Bisnovaty-Kogan, Influence of a plasma on the shadow of a spherically symmetric black hole. *Phys. Rev. D* **92**, 104031 (2015). [arXiv:1507.04217](#) [gr-qc]
32. G.S. Bisnovaty-Kogan, O.Y. Tsupko, Gravitational lensing in presence of plasma: strong lens systems, black hole lensing and shadow. *Universe Ser.* **3**, 57 (2017). [arXiv:1905.06615](#) [gr-qc]
33. B. Cuadros-Melgar, R.D.B. Fontana, J. de Oliveira, Analytical correspondence between shadow radius and black hole quasinormal frequencies. *Phys. Lett. B* **811**, 135966 (2020). [arXiv:2005.09761](#) [gr-qc]
34. K. Jusufi, Correspondence between quasinormal modes and the shadow radius in a wormhole spacetime. *Gen. Relativ. Gravit.* **53**, 87 (2021). [arXiv:2007.16019](#) [gr-qc]
35. K. Jusufi, Connection between the shadow radius and quasinormal modes in rotating spacetimes. *Phys. Rev. D* **101**, 124063 (2020). [arXiv:2004.04664](#) [gr-qc]
36. J.C.S. Neves, Constraining the tidal charge of brane black holes using their shadows. *Eur. Phys. J. C* **80**, 717 (2020). [arXiv:2005.00483](#) [gr-qc]
37. J.C.S. Neves, Upper bound on the GUP parameter using the black hole shadow. *Eur. Phys. J. C* **80**, 343 (2020). [arXiv:1906.11735](#) [gr-qc]
38. S. Chandrasekhar, S.L. Detweiler, The quasi-normal modes of the Schwarzschild black hole. *Proc. R. Soc. Lond. A* **344**, 441–452 (1975)
39. E.W. Leaver, An analytic representation for the quasi-normal modes of Kerr black holes. *Proc. R. Soc. Lond. A* **402**, 285–298 (1985)
40. H.T. Cho, Dirac quasinormal modes in Schwarzschild black hole space-times. *Phys. Rev. D* **68**, 024003 (2003). [arXiv:gr-qc/0303078](#)
41. F.-W. Shu, Y.-G. Shen, Quasinormal modes in Schwarzschild black holes due to arbitrary spin fields. *Phys. Lett. B* **619**, 340–346 (2005). [arXiv:gr-qc/0501098](#)
42. R.A. Konoplya, Quasinormal modes of the Schwarzschild black hole and higher order WKB approach. *J. Phys. Stud.* **8**, 93–100 (2004)
43. H.T. Cho, A.S. Cornell, J. Doukas, T.R. Huang, W. Naylor, A new approach to black hole quasinormal modes: a review of the asymptotic iteration method. *Adv. Math. Phys.* **2012**, 281705 (2012). [arXiv:1111.5024](#) [gr-qc]
44. J.L. Jaramillo, R. Panosso Macedo, L. Al Sheikh, Pseudospectrum and black hole quasinormal mode instability. *Phys. Rev. X* **11**, 031003 (2021). [arXiv:2004.06434](#) [gr-qc]
45. J.P. Boyd, *Chebyshev and Fourier Spectral Methods*, 2nd edn. (Dover Books on Mathematics. Dover Publications, Mineola, 2001)
46. A. Jansen, Overdamped modes in Schwarzschild–de Sitter and a Mathematica package for the numerical computation of quasinormal modes. *Eur. Phys. J. Plus* **132**, 546 (2017). [arXiv:1709.09178](#) [gr-qc]
47. H. Ciftci, R.L. Hall, N. Saad, Asymptotic iteration method for eigenvalue problems. *J. Phys. A* **36**, 11807–11816 (2003)
48. K. Schwarzschild, On the gravitational field of a mass point according to Einstein's theory. *Sitzungsber. Preuss. Akad. Wiss. Berlin (Math. Phys.)* **1916**, 189–196 (1916). [arXiv:physics/9905030](#)
49. C.H. Chen, H.T. Cho, A.S. Cornell, G. Harmsen, Spin-3/2 fields in  $D$ -dimensional Schwarzschild black hole spacetimes. *Phys. Rev. D* **94**, 044052 (2016). [arXiv:1605.05263](#) [gr-qc]
50. V. Shklyar, H. Lenske, U. Mosel, Spin-5/2 fields in hadron physics. *Phys. Rev. C* **82**, 015203 (2010). [arXiv:0912.3751](#) [hep-ph]
51. G.B. Arfken, H.J. Weber, *Mathematical Methods for Physicists*, 4th edn. (Academic Press, San Diego, 1995)
52. F. Tisseur, S. Götzel, The nonlinear eigenvalue problem. MIMS Preprint, 95 (2017). <http://eprints.maths.manchester.ac.uk/id/eprint/2538>
53. R.A. Konoplya, A.V. Zhidenko, Decay of massive scalar field in a Schwarzschild background. *Phys. Lett. B* **609**, 377–384 (2005). [arXiv:gr-qc/0411059](#)
54. P. Grandclement, J. Novak, Spectral methods for numerical relativity. *Living Rev. Relativ.* **12**, 1 (2009). [arXiv:0706.2286](#) [gr-qc]
55. J. Bezanon, A. Edelman, S. Karpinski, V.B. Shah, Julia: a fresh approach to numerical computing. *SIAM Rev.* **59**, 65–98 (2017)
56. L.T. Sanches, 'quasinormalmodes.jl': a julia package for computing discrete eigenvalues of second order odes. *J. Open Source Softw.* **7**, 4077 (2022)
57. H.T. Cho, Asymptotic quasinormal frequencies of different spin fields in spherically symmetric black holes. *Phys. Rev. D* **73**, 024019 (2006). [arXiv:gr-qc/0512052](#)
58. I.B. Khriplovich, G.Y. Ruban, Quasinormal modes for arbitrary spins in the Schwarzschild background. *Int. J. Mod. Phys. D* **15**, 879–894 (2006). [arXiv:gr-qc/0511056](#)
59. V. Ferrari, B. Mashhoon, Oscillations of a black hole. *Phys. Rev. Lett.* **52**, 1361–1364 (1984)
60. M.E.H. Ismail, N. Saad, The asymptotic iteration method revisited. *J. Math. Phys.* **61**, 033501 (2020)
61. F.J. Zerilli, Gravitational field of a particle falling in a Schwarzschild geometry analyzed in tensor harmonics. *Phys. Rev. D* **2**, 2141–2160 (1970)